Materials and Design 74 (2015) 19–24

Contents lists available at ScienceDirect

Materials and Design

journal homepage: www.elsevier.com/locate/matdes

Investigation of resistance heat assisted ultrasonic welding of 6061 aluminum alloys to pure copper

Jingwei Yang, Biao Cao *

School of Mechanical and Automotive Engineering, South China University of Technology, Guangzhou 510640, China

ARTICLE INFO

Article history:
Received 15 November 2014
Revised 12 February 2015
Accepted 28 February 2015
Available online 2 March 2015

Keywords:
Resistance heat assisted ultrasonic welding
Joule effect
Intermetallic compound
Microstructure

ABSTRACT

This paper proposes a new welding method for joining non-ferrous metals: resistance heat assisted ultrasonic welding. Resistance heat generated by the electric Joule effect is used as an additional electrical energy source to assist ultrasonic welding process. A comparison is conducted between two dissimilar Al–Cu joints, one produced by ultrasonic welding and the other by resistance heat assisted ultrasonic welding. In the resistance heat assisted ultrasonic process, the peak power of ultrasonic vibration increases significantly. The interfacial reaction between aluminum and copper is studied as a function of the current. The thickness of the intermetallic compound layer, which is predominantly composed of $CuAl_2$, increases with the current. At a relatively high current (1500 A), resistance heat assisted ultrasonic welding produced a dendritic solidification microstructure at the interface, due to the occurrence of a eutectic reaction, $\alpha\text{-Al} + \theta \rightarrow L$, during the welding process. The influence of current on the mechanical properties of the joints is also discussed.

1. Introduction

Joints of dissimilar materials have a large number of potential industrial applications because of their economic and technical advantages [1]. Copper and aluminum, with their high electrical and thermal conductivity, are preferred in the electronics industries and battery electric vehicles. Hence, a significant amount of Al–Cu joining is needed to transmit electricity. Unfortunately, joining of Al–Cu by conventional fusion welding methods is difficult due to poor weldability, high levels of distortion and rapid formation of bulk intermetallic compound (IMC). Therefore, solid-state welding methods, such as friction stir welding (FSW) [2–4], ultrasonic welding (USW) [5–7], have received much attention as alternative joining techniques for Al–Cu.

FSW is a relatively new solid-state joining technique invented by The Welding Institute (TWI) in 1991 [8]. FSW is demonstrably better than traditional welding technique at joining dissimilar material combinations such as Al–Cu because of its lower temperatures and heat inputs. However, the FSW technique has difficulty meeting with the challenges of the electronics industries and battery electric vehicles, which require the joining of irregular miniature work pieces and multiple dissimilar materials with varying thickness combinations.

Ultrasonic welding is another kind of solid-state joining technique that produces coalescence through high frequency vibration and moderate clamping forces. Although USW has been successfully used for more than 50 years, it has been mainly used in joining thin foils because of the limitation of power of the welding system [5,9–11]. The temperature of the interface is less than 300 °C and very little interfacial interaction happens with most dissimilar material combinations [5,12,13]. Hence, the quality of the joint is not always very high. More recently, with the development of high power USW equipment, much research has been reported on joining thicker similar and dissimilar metal sheets, such as Al–Al, Al–Mg and Al–Fe [14–18]. With higher energy input, the temperature of the weld zone is much higher and an IMC layer is observed at the joint interface. The quality of the joints was effectively improved. From the previous studies, it can be concluded that energy/power is a key factor for dissimilar joints formed by USW, since it affects the growth and size of the IMC layer, which determines the mechanical performance of the joints.

However, the high power USW technique is also difficult to apply to the joining of miniature work pieces. This challenge results from the area of the weld tip, which limits the ultrasonic power delivered in the weld zone. An effective solution to this problem is to utilize an additional form of energy, such as Joule heat, during the USW process. In this study, a new hybrid welding technique, the resistance heat assisted USW (RUSW) technique, is proposed to further contribute to the improvement of USW quality.

* Corresponding author.
E-mail address: mebcao@scut.edu.cn (B. Cao).

http://dx.doi.org/10.1016/j.matdes.2015.02.028
0261-3069/

Sound dissimilar Al–Cu joints were successfully produced by RUSW. The microstructures of the faying surface were analyzed in detail. The influence of the microstructure development on the mechanical properties was also studied.

2. Experimental

As introduced by Cao and Yang [19], RUSW is a hybrid joining technique, as shown in Fig. 1a. The high intensity direct current (DC) flows from the sonotrode, through the contact interface and coupons, and into the anvil where it generates resistance heat by the Joule effect, as depicted in Fig. 1b. Compared with USW, the RUSW technique takes advantage of resistant heat generated by the Joule effect as an additional heat source. Therefore, more heat can be generated in the RUSW process while keeping other parameters, such as welding time and clamping pressure, unchanged. The RUSW system employed was a lateral drive device operating at a frequency of 25 kHz and a maximum output power of 1 kW, which is considered to be a low power USW machine [10,18,20]. The specially designed 3 mm × 3 mm knurled sonotrode (Fig. 1c) was also used as an electrode to deliver the DC. The DC could be adjusted from 0 to 2 kA continuously during the joining process. The ultrasonic energy could be coupled precisely and freely with the DC by the RUSW generator. In this study, ultrasonic energy was synchronized to the DC in the welding process (Fig. 2). The welding time was 0.4 s, the clamping force was 1480 N, and the DC ranged from 1100 to 1500 A.

The joints investigated were produced between 0.3 mm thick 6061 aluminum and 0.3 mm thick copper with no cleaning or surface preparation before welding. The chemical composition (wt.%) of 6061 aluminum is Al–1.3Mg–0.53Si–0.4Fe–0.25Zn–0.33Cu–0.1Mn and the copper is commercially pure C1100 copper. The coupons, which are 75 mm long by 25 mm wide, were welded at the center of the 25 mm overlap.

The vibration amplitude was measured in real time by a KEYENCE LK-G5001 laser displacement sensor and the DC by a CHB-2000SJ Hall current sensor. K-type thermocouples of 0.15 mm diameter were embedded into a machined groove between the 6061 Al and C1100 Cu to measure the temperature of the weld interface, as shown in Fig. 3. Vibration, DC and temperature values were recorded by the NI-6133 data acquisition system.

Microstructural analysis was performed in the cross-section of the joints by using a Hitachi S-3700N microscope complemented by an energy dispersive spectroscopy. The phase constituents of the dissimilar joints were studied by X-ray diffraction (XRD) analysis using a Bruker D8 Advance XRD system. Tensile lap shear tests were carried out at a constant crosshead speed of 1.0 mm/min by using an AGX-50kNXD testing system. A computerized microhardness testing machine was employed for the Vickers microhardness tests diagonally across the cross-section using 25 g load for 15 s.

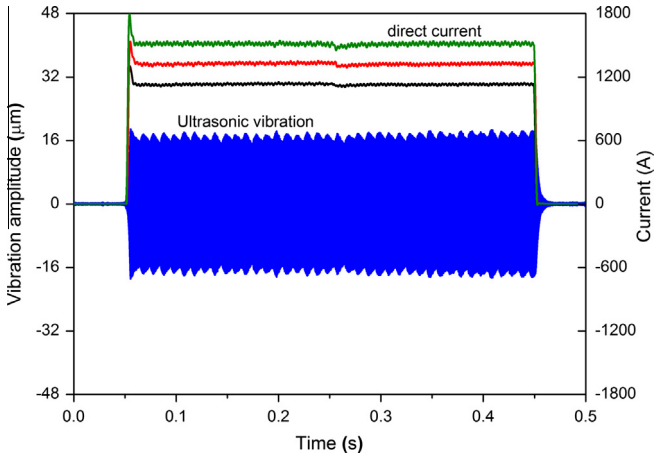

Fig. 2. Hybrid process of ultrasonic vibration and high intensity DC.

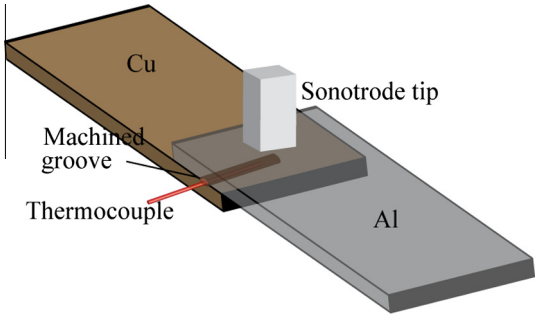

Fig. 3. A schematic demonstrating of the thermal couple position for temperature measurement.

3. Results and discussion

3.1. Ultrasonic power and weld temperatures

The ultrasonic powers of RUSW for various DC inputs are plotted against the time (t), as shown in Fig. 4a. The peak power increased with increasing input DC and reached a maximum of

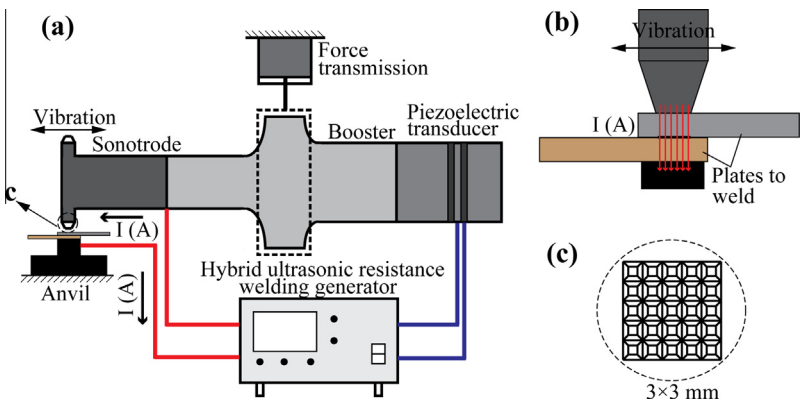

Fig. 1. (a) A schematic diagram of the electric Joule effect assisted ultrasonic welding system, (b) closer detail of the previous and (c) a schematic diagram of the knurled sonotrode tips.

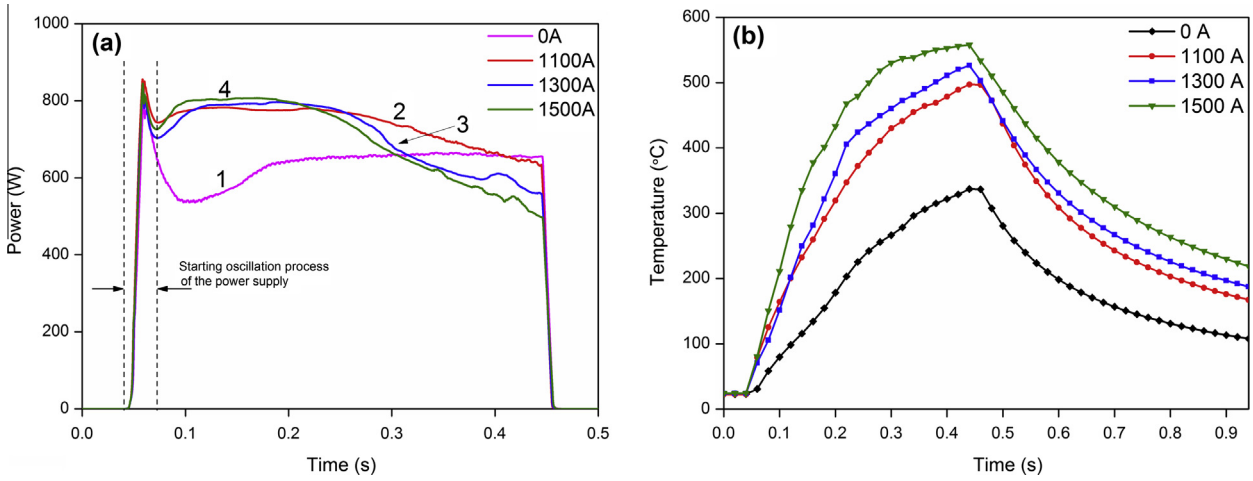

Fig. 4. (a) Ultrasonic power and (b) interfacial temperatures recorded during RUSW with different DC levels.

800 W for a DC of 1500 A. This is more than 30% higher than that without DC input. From Curve 1 in Fig. 4a, it can be noted that the ultrasonic power increases gradually with the welding time and approaches a level of 600 W at $t = 0.2$ s, and then keeps at a steady level until the end of the welding process. In RUSW (Curves 2–4 in Fig. 4a), the ultrasonic power rises quickly to the maximum value at about 0.1 s and holds at this level for about 0.1 s, and thereafter decreases gradually. In the RUSW, a synergic effect is obtained from the two different kinds of welding energy, which takes advantage of the beneficial aspects of each process and minimizes the shortcomings of each other in order to maintain a more consistent power throughout the whole welding time [21]. Because of the resistance heat generated by Joule effect, the temperature of the metal rises. As a result, the ductility of the metals increases and the deformation resistance decreases, which could improve the viscoplasticity of the welded metals. This promotes the ultrasonic welding at the initial stage of the process. On the other hand, with the temperature rising to some threshold, the material flow stress becomes very small, which will allow the sonotrode to oscillate much more easily. As a result, less power will be required from the power generator.

To further understand the welding process and interface evolution, the temperatures were measured by using a thin (0.15 mm) thermocouple embedded at the center of weld zone through a groove precisely machined in the 6061 specimens. The temperature data are depicted in Fig. 4b. The peak temperature increases with increasing DC. The maximum interfacial temperature reached at the input DC of 1500 A is about 558 °C in RUSW, which is higher than the melting point (548 °C) of Al–Cu eutectic alloy. Further, the heating rate is much higher in RUSW than in USW. However, the heating rate decreases with increasing welding time in RUSW. This slowdown is mainly determined by the ultrasonic power and the contact resistance between the tip and the anvil. At the initial stage, both the ultrasonic power and contact resistance are high, and consequently, more energy is delivered into the weld zone. With prolonged welding time, the input energy is reducing and the dissipation rate is increasing. Hence, the heating rate is reduced.

3.2. Microstructural evolution

The effect of the DC on the microstructural evolution of the welding interface through the center of the dissimilar joints was studied. The SEM micrographs, acquired in back scattered electrons (BSE) mode, of selected cross-section areas of the Al–Cu joints formed with different DC levels, are illustrated in Fig. 5. An IMC layer is clearly visible at the faying surface of the RUSW (Fig. 5b, c and e). However, a diffusion reaction could hardly be observed in the weld formed by using only ultrasonic power (Fig. 5a). With the same weld area, the coupons could not be joined without ultrasonic energy even if the DC reached 1500 A.

It can be seen from Fig. 5b that at the input DC level of 1100 A, an IMC layer growing mainly out of the Al side is distributed continuously along the welding interface. The thickness of the reaction layer was approximate 2 μm. With higher DC input, the average thickness of the IMC layer increased and reached about 8 μm at a DC level of 1300 A (Fig. 5c). At this DC level, the IMC layer is composed of two discernible sub-layers (marked as A and B in Fig. 5c). The average thickness was 1 μm and 7 μm for A and B, respectively. When the input current reached 1500 A, progressive diffusion reactions dilated the interface to 20 μm thick and clear evidence of melting could be observed along the welding interface.

EDS analysis has been performed to identify the IMC phases formed along the interface of the dissimilar joints. The results of EDS line-scan analysis of Fig. 5c are shown in Fig. 5d. Both the Cu and Al curves across the IMC layer present a plateau (Fig. 5d), which indicates that the reaction layer is probably composed of a single IMC phase. The chemical composition (wt.%) at points C is 56.91Cu–43.09Al. This means that the IMC layer is mainly composed of $CuAl_2$ according to the Al–Cu phase diagram [22].

XRD analysis was carried out on both fracture surfaces of 6061 aluminum and copper after the tensile lap shear tests for joints produced at the DC level of 1300 A. The results confirm that the Al–Cu welds consist only one intermetallic phase: $CuAl_2$ (Fig. 6). Similar results have been reported by other researchers in USW [6,7] and Xue et al. in FSW [4] of 6061 aluminum to copper.

In RUSW, as the current flowed through the metals between the weld tip and the anvil, heat first was generated at the micro-contacts by the electric Joule effect and friction. This causes the plastic deformation resistance of the micro-contacts to decrease substantially, which is a favoring factor for the ultrasonic welding. On the other hand, the dynamic changes of the micro-contacts induced by ultrasonic vibration will also influence the heat generation. Owing to the complex synergistic effects between the ultrasonic energy and resistance heat, the temperature of the interface rises rapidly (Fig. 4b), which causes significant inter-diffusion in the micro-weld zones. When the diffusion reaches a critical point, the nucleation of the IMC will occur within the first locally welded points. With increasing DC intensity, the IMC layer grows along the interface and grows thicker until a continuous IMC layer is formed (Fig. 5b and c).

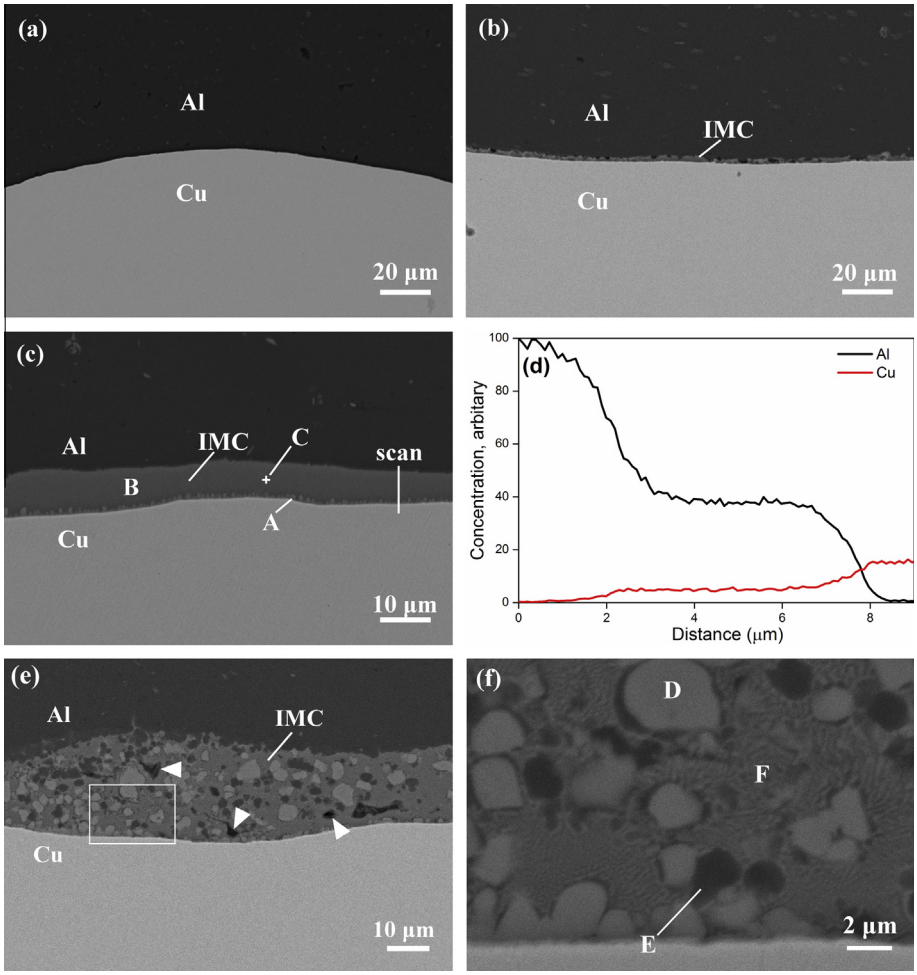

Fig. 5. SEM images of the joins obtained under DC intensity of : (a) 0 A, (b) 1100 A, (c) 1300 A, (e) 1500 A; and (f) magnified view of the highlighted area in (e); (d) EDS line-scan across the layer at DC of 1300 A.

Although the welding time is only 0.4 s and the peak temperatures are 497 °C (Fig. 4b) for DC values of 1100 A, the average thickness of the IMC layer has grown to 2 μm (Fig. 5b). This strongly suggests that the growth rate of the reaction layer in the RUSW is much more rapid than that for static growth. It is reasonable that the diffusion between Al and Cu will be accelerated by the following two factors in RUSW: first, an increase in temperature caused by the Joule heat and plastic deformation of the faying surface; second, an increase in the concentrations of lattice defects such as vacancies, dislocations and grain boundaries as explained below.

From Fig. 4b, it can be seen that the difference in the peak temperatures is only about 30 °C, as the DC is increased from 1100 A to 1300 A. Despite this small difference, the average thickness of the IMC layer has increased from 2 μm to 8 μm (Fig. 5c). It seems that higher temperatures cannot solely account for the rapid growth of the IMC layer. Thus, a second factor must be having a great influence on the rapid growth of the IMC layer. In RUSW, under the ultrasonic vibration and resistance heat, the strain rate and the accumulated stain are very high, even though the welding process is short. Consequently, severe plastic deformation concentrates mainly at the faying surface. It has been reported by Divinski et al. [23] and Oh-ishi et al. [24] that during the process of severe plastic deformation, high densities of vacancies and dislocations are formed, along with large fractions of high angle boundaries. It is well accepted that a high density of lattice defects will dramatically enhance the diffusion rate because the activation energy

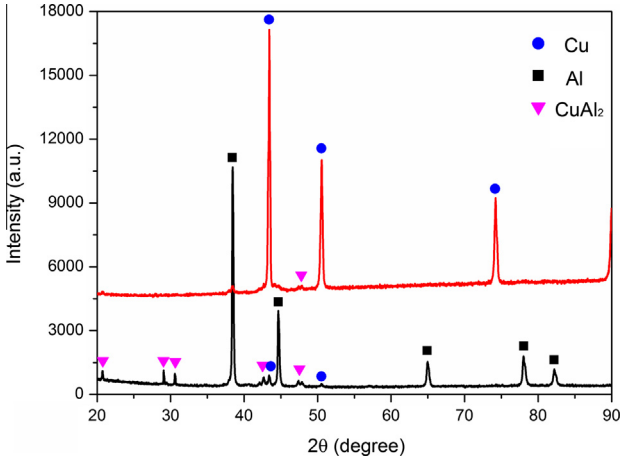

Fig. 6. XRD patterns obtained from the weld fracture surface of the sample by RUSW at 1300 A DC input.

for diffusion along the dislocation or grain boundary is just 50–70% of that for lattice diffusion [24]. Therefore, it can be concluded that in RUSW, in addition to the temperature, the severe dynamic plastic deformation caused by the ultrasonic energy and resistance heat also plays an important role on accelerating the intermetallic reaction kinetics.

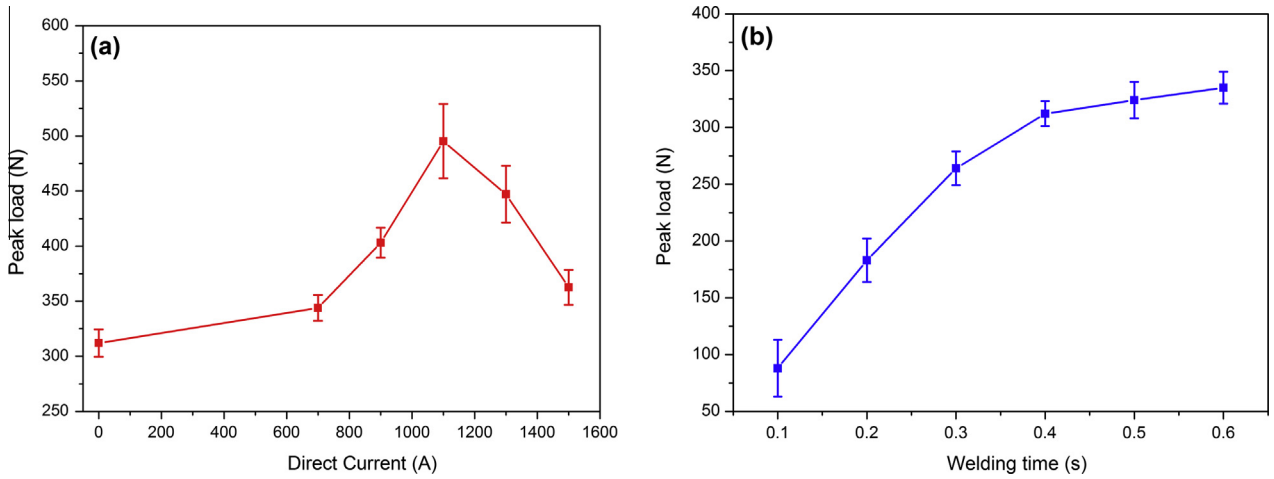

Fig. 7. Lap shear test results of: (a) RUSW joints as a function of DC intensity and (b) USW joints as a function of welding time.

When the input DC reached 1500 A, the peak temperature recorded at the welding surface is up to 558 °C, higher than the melting point of the Al–Cu eutectic alloy. Evidence of solidified microstructure was also observed at the weld interface. The microstructure is comprised of some cavities (arrows) and three distinguished regions D, E and F, as revealed in Fig. 5e and f. Region D consists of only a white phase and E a black one, while region F has a hypoeutectic microstructure consisting of the two phases. The microstructures of D and F were significantly different from the two parent metals. Quantitative analysis of the chemical composition (wt.%) by EDS showed that the region D in Fig. 5f consisted of 53.31Cu–46.69Al, while the region F contained 26.89Cu–73.11Al, which indicates that the regions D and F (in Fig. 5f) are $CuAl_2$ and a hypoeutectic structure composed of α-Al and $CuAl_2$, respectively. This means that the eutectic reaction $\alpha\text{-Al} + \theta \rightarrow L$ has occurred along the interface.

3.3. Mechanical properties

The results of the peak lap shear tensile loads for RUSW joints at different DC intensities and for USW joints formed with different welding times are shown in Fig. 7a and b, respectively. Clearly, the lap shear strength has a great improvement as the USW process was assisted by the DC. The peak load increases with increasing DC value, and reaches a maximum value of 530 N at the DC level of 1100 A, and then decreases gradually.

Apparently, the peak lap shear loads of the dissimilar Al–Cu joints were influenced by the growth of the IMC layer between Al and Cu at the faying surface. It is well known that in dissimilar joints the presence of IMCs is an indication of sound metallurgical joining. A thin, uniform and continuous IMC layer is an essential requirement for sound joining [25]. Hence, the good metallurgical joining between Al and Cu produced by RUSW was attributed to the formation of the continuous and uniform IMC layer with a proper thickness of 2 μm. However, the previous studies have indicated that when the IMC layer became too thick, the mechanical properties would suffer [25]. Obviously, excessive IMCs generated in RUSW at the faying surface are the reason for the reduced lap shear load of the joints produced with higher DC input.

In USW, as it is shown in Fig. 7b, the peak lap shear loads increase rapidly with increasing welding time before reaching a plateau. However, the maximum value of the lap shear load is only about 340 N. During the initiation stage, the frictional forces between the weld interfaces cause surface asperities to progressively shear and plastically deform, which in turn breaks the contaminants surrounding the asperities and result in discrete areas of metal-to-metal adhesion. Then, the microbonds increase in size and density over the weld zone. Because of the low power of ultrasonic welding, the resulting diffusion reaction layer was so thin that it could hardly be observed. This means that the weld strength is mainly determined by the effective net area of the microbonds. Based on this, it is possible to conclude that the difference of the weld strength between low power USW and RUSW is attributable to their different characteristic joining mechanism.

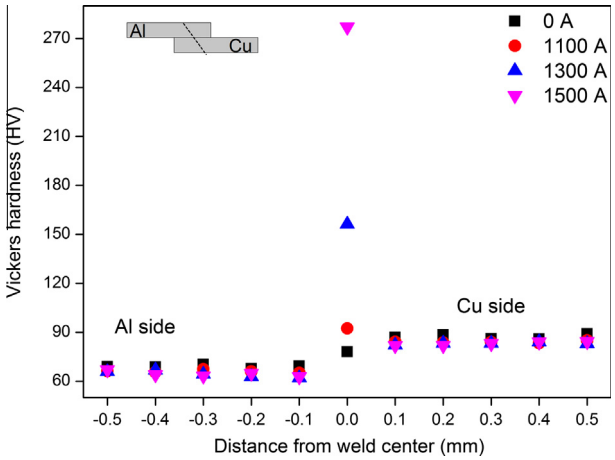

Fig. 8. Vickers microhardness profile measured across the welded joints under different intensity DC.

The microhardness of the Al–Cu joints by RUSW with different DC inputs, which was measured diagonally from the weld center toward the edge of the joint, is shown in Fig. 8. The microhardness of Al and Cu in the weld zone is softer than the parent metals, 75 Hv for 6061-T4 aluminum and 95 Hv for copper. It is reasonable that with the increase of the temperature, grain growth occurs, causing a decrease in hardness as discovered by Hall [26]. The microhardness at the center of the faying surface was much higher compared to the parent metals because of the hard and brittle property of the $CuAl_2$.

4. Conclusions

The resistance heat assisted ultrasonic welding technique (RUSW) was proposed in the paper. RUSW of 6061 aluminum to pure copper was investigated via comparison with the ultrasonic

welding (USW) process when holding the welding parameters constant. The following conclusions can be drawn:

1. Due to the synergistic effects of the ultrasonic energy and resistance heat, the peak power of ultrasonic vibration and the peak temperature of the weld interface are increased significantly in RUSW.
2. A thin, uniform, and continuous IMC layer was observed at the faying surface when the DC reached 1100 A. The IMC layer increases rapidly with increasing the DC values. As the DC increased to 1500 A, evidence of a solidified microstructure was observed at the weld interface. Both the EDS and XRD results confirm that the IMC layer is mainly composed of $CuAl_2$.
3. The intermetallic reaction layer resulted in a good metallurgical bonding and increased the mechanical properties of the Al–Cu dissimilar joints. The lap shear load reached a maximum value of 550 N at the DC level of 1100 A, while for USW the maximum lap shear load was much lower (about 300 N).

Acknowledgement

This research was supported by the National Natural Science Foundation of China under Grant No. 51175184.

References

[1] Z. Sun, Joining dissimilar material combinations: materials and processes, Int. J. Mater. Prod. Technol. 10 (1) (1995) 16–26.
[2] H. Bisadi, A. Tavakoli, M.T. Sangsaraki, K.T. Sangsaraki, The influences of rotational and welding speeds on microstructures and mechanical properties of friction stir welded Al5083 and commercially pure copper sheets lap joints, Mater. Des. 43 (2013) 80–88.
[3] J.Q. Zhang, Y.F. Shen, X. Yao, H.S. Xu, B. Li, Investigation on dissimilar underwater friction stir lap welding of 6061-T6 aluminum alloy to pure copper, Mater. Des. 64 (2014) 74–80.
[4] P. Xue, D.R. Ni, D. Wang, B.L. Xiao, Z.Y. Ma, Effect of friction stir welding parameters on the microstructure and mechanical properties of the dissimilar Al–Cu joints, Mater. Sci. Eng. A 528 (2011) 4683–4689.
[5] S. Matsuoka, H. Imai, Direct welding of different metals used ultrasonic vibration, J. Mater. Process. Technol. 209 (2) (2009) 954–960.
[6] R. Balasundaram, V.K. Patel, S.D. Bhole, D.L. Chen, Effect of zinc interlayer on ultrasonic spot welded aluminum-to-copper joints, Mater. Sci. Eng. A 607 (2014) 277–286.
[7] J.W. Yang, B. Cao, X.C. He, H.S. Luo, Microstructure evolution and mechanical properties of Cu–Al joints by ultrasonic welding, Sci. Technol. Weld. Join. 19 (6) (2014) 500–504.
[8] W.M. Thomas, E.D. Nicholas, J.C. Needham, M.G. Murch, P.T. Smith, C.J. Dawes, GB Patent Application No. 9125978.8, 1991.
[9] E.A. Neppiras, Ultrasonic welding of metals, Ultrasonics 3 (3) (1965) 128–135.
[10] M. Komada, Ultrasonic welding of non-ferrous metals, Weld. Int. 3 (10) (1989) 853–860.
[11] I.E. Gunduz, T. Ando, E. Shattuck, P.Y. Wong, C.C. Doumanidis, Enhanced diffusion and phase transformations during ultrasonic welding of zinc and aluminum, Scripta Mater. 52 (9) (2005) 939–943.
[12] Z.Q. Zhu, K.Y. Lee, X.L. Wang, Ultrasonic welding of dissimilar metals, AA6061 and Ti6Al4V, Int. J. Adv. Manuf. Technol. 59 (5–8) (2012) 569–574.
[13] G. Flood, Ultrasonic energy welds copper to aluminum, Weld. J. 76 (1) (1997) 43–45.
[14] D. Bakavos, P.B. Prangnell, Mechanisms of joint and microstructure formation in high power ultrasonic spot welding 6111 aluminium automotive sheet, Mater. Sci. Eng. A 527 (2010) 6320–6334.
[15] A. Panteli, J. Robson, I. Brough, P.B. Prangnell, The effect of high strain rate deformation on intermetallic reaction during ultrasonic welding aluminium to magnesium, Mater. Sci. Eng. A 556 (2012) 31–42.
[16] A. Panteli, Y.C. Chen, D. Strong, X.Y. Zhang, P.B. Prangnell, Optimization of aluminium-to-magnesium ultrasonic spot welding, JOM 64 (3) (2012) 414–420.
[17] P.B. Prangnell, F. Haddadi, Y.C. Chen, Ultrasonic spot welding of aluminium to steel for automotive applications – microstructure and optimization, Mater. Sci. Technol. 27 (3) (2011) 617–624.
[18] F. Haddadi, Rapid intermetallic growth under high strain rate deformation during high power ultrasonic spot welding of aluminium to steel, Mater. Des. 66 (2015) 459–472.
[19] B. Cao, J.W. Yang, CN Patent Application No. 201010280073.2, 2012.
[20] Y.C. Chen, D. Bakavos, A. Gholinia, P.B. Prangnell, HAZ development and accelerated post-weld natural ageing in ultrasonic spot welding aluminium 6111-T4 automotive sheet, Acta Mater. 60 (6) (2012) 2816–2828.
[21] T.G. Santos, R.M. Miranda, P. Vilac, Friction Stir Welding assisted by electrical Joule effect, J. Mater. Process. Technol. 214 (10) (2014) 2127–2133.
[22] Y. Funamizu, K. Watanabe, Interdiffusion in the Al–Cu system, Trans. Jpn. Inst. Metal 12 (3) (1971) 147–152.
[23] S.V. Divinski, G. Reglitz, H. Rösner, Y. Estrin, G. Wilde, Ultra-fast diffusion channels in pure Ni severely deformed by equal-channel angular pressing, Acta Mater. 59 (5) (2011) 1974–1985.
[24] K. Oh-ishi, K. Edalati, H.S. Kim, K. Hono, Z. Horita, High-pressure torsion for enhanced atomic diffusion and promoting solid-state reactions in the aluminum–copper system, Acta Mater. 61 (9) (2013) 3482–3489.
[25] T. Laurila, V. Vuorinen, J.K. Kivilahti, Interfacial reactions between lead-free solders and common base materials, Mater. Sci. Eng. R-Rep. 49 (1) (2005) 1–60.
[26] E.O. Hall, Variations of hardness of metal with grain size, Nature 173 (1954) 948–949.